Cancer Science
Japanese Cancer Association JCA
Open Access

Spread of tumor microenvironment contributes to colonic obstruction through subperitoneal fibroblast activation in colon cancer

Mitsuru Yokota,[1,2] Motohiro Kojima,[3] Youichi Higuchi,[4] Yuji Nishizawa,[1] Akihiro Kobayashi,[1] Masaaki Ito,[1] Norio Saito[1] and Atsushi Ochiai[3]

[1]Division of Colorectal Surgery, Research Center for Innovative Oncology, National Cancer Center Hospital East, Kashiwa; [2]Department of Surgery, School of Medicine, Keio University, Tokyo; [3]Division of Pathology, Research Center for Innovative Oncology, National Cancer Center Hospital East, Kashiwa; [4]Laboratory of Cancer Biology, Department of Integrated Biosciences, Graduate School of Frontier Sciences, The University of Tokyo, Tokyo, Japan

Key words

Colon cancer, elastic laminal invasion, fibroblast, obstruction, tumor microenvironment

Correspondence

Atsushi Ochiai, Division of Pathology, Research Center for Innovative Oncology, National Cancer Center Hospital East, 6-5-1 Kashiwanoha, Kashiwa 277-8577, Japan.
Tel: +81-4-7133-1111; Fax: +81-4-7131-9960;
E-mail: aochiai@east.ncc.go.jp

Funding Information

Japan Society for the Promotion of Science.

Received November 4, 2014; Revised January 3, 2015; Accepted January 14, 2015

Cancer Sci **106** (2015) 466–474

doi: 10.1111/cas.12615

We evaluated the influence of the cancer microenvironment formed by peritoneal invasion (CMPI) on clinical findings in colon cancer patients. In addition to the association with poor prognosis, we discovered a relationship with bowel obstruction. Detailed analysis revealed that clinical findings related to bowel obstruction occurred more frequently in patients with an elevated type tumor, which had peritoneal elastic laminal elevation to the tumor surface, compared to those with non-elevated type tumors among those with elastic laminal invasion (ELI). Lateral tumor spread and increase of tumor annularity rate in ELI-positive elevated type cases suggested the morphological progression from ELI-positive non-elevated type to elevated type. In addition, α-smooth muscle actin expression was the highest in ELI-positive elevated type, and prominent expressions were found not only in the deep tumor area but also in the shallow tumor area. Furthermore, contraction assays revealed the robust contractile ability of subperitoneal fibroblasts stimulated by cancer cell-conditioned medium. Our findings suggest that CMPI spread into the luminal side of the colonic wall along with tumor progression, which caused bowel obstruction through the activation of subperitoneal fibroblasts. However, although the clinical outcome was not different between the two types, the clinical findings were affected by the spread of CMPI. We are the first to explore how the alteration of the tumor-promoting microenvironment, along with tumor progression, contributes to the development of clinical findings.

Colorectal cancer (CRC) is one of the most frequent malignancies in the world.[1–3] The majority of patients with early stage CRC have no symptoms and their cancers are often detected during colorectal screening. However, in spite of the development of the screening system, there are still many patients whose cancers are diagnosed in an advanced stage with clinical findings such as melena, abdominal pain, or obstruction.[4,5] Clinical findings related to CRC are caused by tumor growth into the intestinal lumen and tumor invasion to the adjacent organs, therefore the development of clinical findings typically occurs in relatively advanced stage CRC. Nevertheless, not all patients with advanced stage CRC experience clinical findings. For instance, patients with an apple-core lesion on barium enema examination do not always show obstructive symptoms and there may be no difficulty in passage of the colonoscope despite a typical annular severe stricture formation. Thus, the relationship between clinical findings and tumor progression remains unclear.

Recently, peritoneal elastic laminal invasion (ELI) was reported to be a strong prognostic factor in colon cancer (CC).[6–8] Furthermore, we reported that the cancer microenvironment formed by the peritoneal invasion (CMPI) promoted tumor progression and metastasis through the interaction between subperitoneal fibroblasts (SPFs) and cancer cells.[9] Peritoneal tissue is one of the final layers of the colonic wall, so ELI occurred in advanced stage CC. In addition, marked morphological and pathological alterations were observed in tumor tissues after ELI. Therefore, ELI, and CMPI formed after ELI, may cause CC-related clinical findings. In this study, we aimed to evaluate how the formation of the tumor microenvironment, such as CMPI, could change the characteristics of the tumor tissue, and whether it could affect clinical findings. Using detailed morphometrical and biological investigation, we evaluated the interaction between SPFs and cancer cells within CMPI in colonic obstruction.

Materials and Methods

Patient selection and follow-up. A total of 205 patients with pT3 and pT4a CC who underwent curative surgery at the National Cancer Center Hospital East (Kashiwa, Japan) between January 2007 and December 2010, were retrospectively evaluated (Fig. 1). Demographics, clinical symptoms

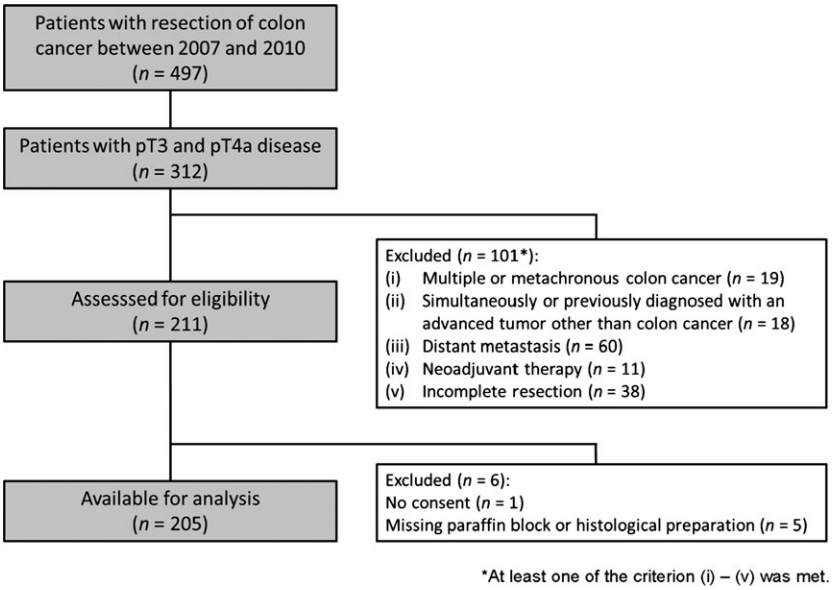

Fig. 1. Flow diagram of the study of colon cancer patients with pT3 and pT4a disease who underwent curative surgery between January 2007 and December 2010. *At least one of the criteria (i–v) was met.

and treatments, serum data, colonoscopy findings, and histopathology and prognostic outcome data for the patients were recorded. Clinical symptoms included abdominal pain, abdominal distension, and vomiting. Treatment of bowel obstruction, including fasting and infusion or decompression with an ileus tube, was carried out according to the severity of the patient's condition. No passage of colonoscope was defined as the inability of an experienced endoscopist to pass a thin scope (φ11.5 mm) beyond a tumor site to the oral-sided colon, and was recorded as one of the features of bowel obstruction.

All cases were reclassified based on the 7th edition of the Union for International Cancer Control TNM staging system.[10] We did not categorize isolated tumor deposits as lymph node metastases to evaluate independently. Follow-up after surgery was carried out in all patients and was comprised

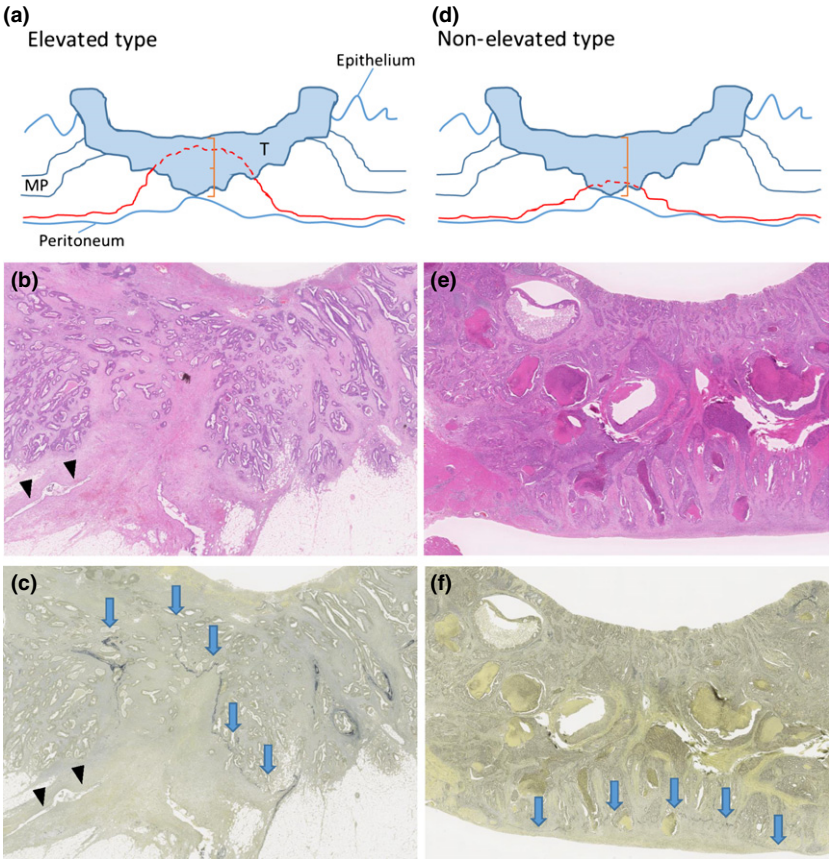

Fig. 2. Two types of elastic lamina invasion (ELI)-positive cases of colon cancer. ELI-positive cases were divided into elevated type (a) and non-elevated type (d) based on whether or not the peritoneal elastic lamina (PEL) was elevated to the surface by more than half the distance of the tumor invasion. H&E staining (b, ×20) and elastica staining (c, ×20) of the elevated type. H&E staining (e, ×20) and elastica staining (f, ×20) of the non-elevated type. Red line represents PEL (a, d). Arrow heads indicate cleft (b, c). Arrows indicate PEL (c, f). MP, muscularis propria; T, tumor.

of serum tumor marker measurement every 3 months and chest and abdominal computed tomography (CT) every 6 months for the first 3 years, then every 6 months for the next 2 years. All patients were followed up from the date of surgery to the last contact (death or last follow-up). Metastasis and local recurrence were considered as tumor recurrence, and the final diagnosis was made by imaging (CT, magnetic resonance imaging, and/or PET-CT), cytology, or biopsy.

Written informed consent for tissue collection and use for research was obtained. The conduct of the study was approved by our local ethics committee (National Cancer Center Hospital; no. 2013-293).

Histopathological analysis. We used the same histopathological examination protocol as that used in our previous study.[6] The resected specimens were fixed in 10% formalin, and the entire tumor was cut into 5-mm slices. Representative slices were embedded in paraffin, cut into 3-μm sections and stained with H&E and elastica stain to evaluate ELI status and lymphovascular invasion. Because of discrimination of the peritoneal elastic lamina (PEL) from the retroperitoneal fascia, we confirmed the continuity from the PEL found at the other area of colonic wall. Therefore, we undertook elastica stain on at least one whole slice where the tumor was closest to the peritoneal surface. The median numbers of H&E and elastica stained sections were 8.0 (range, 2–27) and 5.0 (range, 2–16), respectively.

Cases with tumor invasion beyond the PEL were defined as ELI-positive. First, we divided patients into ELI-positive and ELI-negative cases to identify the difference of clinical features based on the ELI status. Additionally, ELI-positive cases were divided into elevated type or non-elevated type. Cases with the PEL elevation to the surface of more than half the distance of the tumor invasion were regarded as ELI-positive elevated type (Fig. 2). Then, the association between the clinicopathological findings and the three tumor types (ELI-negative, ELI-positive non-elevated type, and ELI-positive elevated type) were assessed.

Azan staining, immunohistochemistry, and computer-assisted image analysis. Two consecutive sections of 4-μm thick slices were obtained from paraffin-embedded blocks, which included all layers of the intestinal wall and tumor area with the deepest infiltration. One section was used for immunohistochemical α-smooth muscle actin (α-SMA) staining (×200, clone 1A4; Dako, Carpinteria, CA, USA) and the other for Azan staining. Immunostaining was carried out using an autostainer (Ventana Benchmark; Roche Diagnostics, Tokyo, Japan), as described previously.[9] High-resolution slide images from each H&E, α-SMA, and Azan stained section were obtained using a Nano Zoomer 2.0-HT slide scanner (Hamamatsu Photonics, Hamamatsu, Japan). All sections were examined using viewer software (NDP View; Hamamatsu Photonics). We divided the tumor area into two equal parts of shallow and deep areas. Five fields with the highest α-SMA and Azan expressions were randomly selected from the shallow and deep layer of each tumor (a total of 10 fields per specimen). Then, images of ×40 magnification (0.59 mm^2) were saved as JPEG files. The ratios of the α-SMA and Azan positive area in the images were calculated using morphometric software (WinRoof; Mitani, Fukui, Japan), as described previously.[9]

Cell cultures and cell lines. Both SPFs and submucosal fibroblasts (SMFs) were obtained from normal sigmoid colon tissue of three patients operated on for sigmoid CC as described previously.[9] The samples were routinely maintained in MF-medium (Toyobo, Tokyo, Japan) at 37°C in a humid atmosphere containing 5% CO_2.

The human colonic cancer cell line DLD-1 was obtained from ATCC (Manassas, VA, USA), and maintained in DMEM (Sigma-Aldrich, St. Louis, MO, USA) containing 100 U/mL penicillin and 100 μg/mL streptomycin (Sigma-Aldrich) and 10% FBS (Gibco, Palo Alto, CA, USA).

Preparation of cancer cell-conditioned medium. Cancer cell-conditioned medium (CCCM) from DLD-1 was obtained as described previously.[9] Initially, $1.7 \times 10^4/cm^2$ of DLD-1 was grown in maintained medium for 48 h, and then starved in DMEM for 24 h. The medium was removed and used as CCCM.

Collagen gel contraction assay. A standard kit assay was used to investigate the difference of contractile ability in fibroblasts (Cell Biolabs, San Diego, CA, USA).[11] Briefly, $1.0 \times 10^5/mm^3$ fibroblasts were mixed with a cold collagen gel solution, then 0.5 mL fibroblast–collagen mixture was added per well in a 24-well plate, and incubated for 1 h at

Table 1. Clinical characteristics according to elastic laminal invasion (ELI) status in patients who underwent primary resection for pT3 and pT4a colon cancer (*n* = 205)

	ELI(−) *n* = 113	ELI(+) *n* = 92	*P*-value
Age, years			
Median (range)	68 (24–90)	64 (38-89)	0.051
Sex			
Male	51	46	0.488
Female	62	46	
Body mass index, kg/m^2			
Median (range)	23.3 (16.2–34.2)	22.5 (14.5–39.3)	0.141
Total protein level, g/dL			
Median (range)	6.8 (5.4–7.9)	6.8 (5.2–7.9)	0.886
Albumin level, g/dL			
Median (range)	4.1 (2.4–4.8)	4.0 (2.7–5.0)	0.821
C-reactive protein level, mg/dL			
Median (range)	0.10 (0.01–6.46)	0.12 (0.01–5.10)	0.867
White blood cell count, $/mm^3$			
Median (range)	5700 (3200–11 800)	5850 (3200–12 000)	0.571
Neutrophil count, $/mm^3$			
Median (range)	3429 (1728–8626)	3485 (1141–9821)	0.551
Lymphocyte count, $/mm^3$			
Median (range)	1693 (776–3493)	1736 (773–5064)	0.758
Hemoglobin concentration, g/dL			
Median (range)	12.7 (6.9–17.7)	12.7 (7.6–16.7)	0.712
CEA level, ng/mL			
Median (range)	3.6 (0.6–358.9)	3.4 (0.7–197.0)	0.401
Tumor location			
Right	40	22	0.193
Transverse	17	18	
Left	56	52	
Abdominal symptoms			
+	25	34	0.020
−	88	58	
Passage of colon colonoscope†			
+	91	50	<0.001
−	19	41	
Treatment of bowel obstruction			
+	2	11	0.003
−	111	81	

CEA, carcinoembryonic antigen. †Four patients were missing data.

37°C. After the gel polymerization, 1 mL DMEM containing 100 U/mL penicillin, 100 μg/mL streptomycin, and 10% FBS was added and incubated for 24 h. Next, the medium was removed from the plate, and CCCM was added to three wells of each fibroblast type. As a control, serum-free DMEM was added to another three wells. Twenty-four hours later, each gel was gently released from the sides of wells, and pictures were taken another 48 h later. The area of the gel was measured using morphometric software (WinRoof; Mitani), and the contraction rate was obtained by the division of the gel area with CCCM stimulation by the initial gel area.

Statistical analysis. Differences in the clinicopathological features between ELI-positive and ELI-negative cases were assessed using Fisher's exact test and the Mann–Whitney *U*-test; α-SMA and Azan positive area ratios were compared using Student's *t*-test.

Recurrence-free survival (RFS) was defined as the time that elapsed between the date of surgery and any relapse or the last contact. Kaplan–Meier survival curves were plotted and compared using the log–rank test.

All statistical analyses were carried out using SPSS 22 (SPSS, Chicago, IL, USA). All *P*-values were reported as two sided, and statistical significance was defined as $P < 0.05$.

Results

Association between clinical characteristics and ELI status. In the dataset, 92 patients (44.9%) were identified as ELI-positive. Serum data, nutritional status, level of tumor marker, and tumor location were not associated with ELI status (Table 1). However, patients with ELI-positive tumors more frequently complained of clinical symptoms and required treatment for bowel obstruction. No passage of the colonoscope was also found more frequently in ELI-positive cases. For a detailed analysis, dividing ELI-positive cases into two types, clinical findings related to bowel obstruction were found more frequently in the ELI-positive elevated type than in the ELI-positive non-elevated type cases (Fig. 3). Furthermore, patients with ELI-positive elevated type tumors required more treatment for bowel obstruction compared to patients with ELI-negative or ELI-positive non-elevated type tumors.

Association between histopathological characteristics and ELI status. Thirty-eight percent of patients with pT3 disease ($n = 70$) and all patients with pT4a disease ($n = 22$) were ELI-positive. Histopathological findings by tumor type are shown in Table 2. Thin ulcers and thickening under the muscular layer were identified as morphological changes associated with an ELI-positive state. The ELI-positive type was also significantly associated with an invasive infiltrating pattern, a higher pathological nodal stage, a high budding grade, a high lymphovascular invasion grade, and a high perineural invasion grade; features that are related to tumor malignancy. Furthermore, tumor size and annularity rate significantly increased in the ELI-positive elevated type cases. These clinicopathological results suggested that elevation of PEL was associated with bowel obstruction and occurred in parallel with tumor progression.

Association between fibrosis and ELI status. Fibrosis in CRC is associated with bowel obstruction.[12–14] Therefore, we quantitatively assessed fibrosis in tumor tissue using morphometry on Azan and α-SMA staining, which was evaluated by tumor type.

The α-SMA expression was higher in order of ELI-positive elevated type, ELI-positive non-elevated type, and ELI-negative

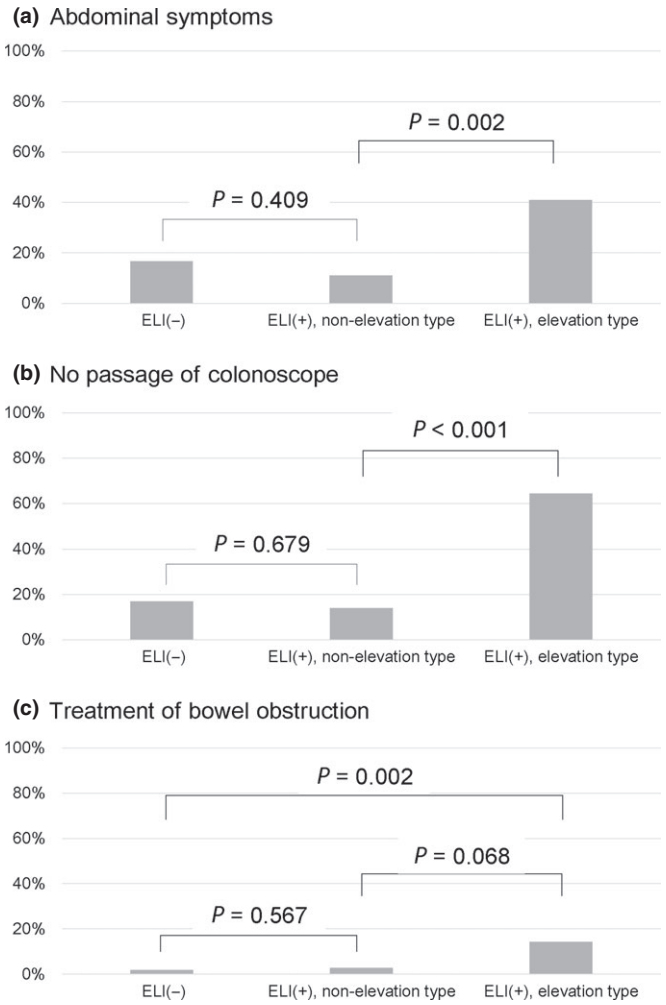

Fig. 3. Incidence rates of clinical findings by colon cancer tumor type. Clinical findings included abdominal symptoms (a), no passage of the colonoscope (b), and treatment of bowel obstruction (c). Tumor types were divided into elastic lamina invasion (ELI)-negative type, elevated type ELI-positive cases, and non-elevated type ELI-positive cases.

cases (Fig. 4a,b). An increase of α-SMA positive area ratio was strongly associated with ELI status, and it was observed not only in the deep tumor area but also in the shallow tumor area. Furthermore, there was a significant difference in the ratio between ELI-positive elevated type and ELI-positive non-elevated type, especially in the shallow tumor area. In the Azan stain, the fibrosis area was also higher in ELI-positive cases than in ELI-negative cases, but the ratio was not different between ELI-positive elevated type and ELI-positive non-elevated type (Fig. 4a,c).

Association between prognosis and ELI status. The median follow-up was 4.3 years (range, 0.3–6.6 years). The 3-year RFS rates for ELI-negative and ELI-positive patients were 95.4% and 74.9%, respectively, and the log–rank analysis revealed a statistically significant difference ($P < 0.001$; Fig. 5a). However, the 3-year RFS rates for ELI-positive non-elevated type and ELI-positive elevated type were 72.2% and 76.7%, respectively, and there was no significant difference between these two types among ELI-positive patients ($P = 0.340$; Fig. 5b).

Contractile ability of SPFs. To estimate the contribution of SPFs to bowel obstruction, contraction assays were carried out and contractile abilities were compared with those of SMFs.

Table 2. Clinical and histopathological findings by tumor type in patients who underwent primary resection for pT3 and pT4a colon cancer (*n* = 205)

	1. ELI(−) *n* = 113	2. ELI(+) Non-elevated type *n* = 36	3. ELI(+) Elevated type *n* = 56	*P*-value (1. *vs* 2.)	*P*-value (2. *vs* 3.)
Maximum transverse tumor size, cm					
Median (range)	4.0 (1.0–10.0)	3.4 (1.0–9.2)	5.0 (2.0–10.5)	0.250	0.003
Maximum longitudinal tumor size, cm					
Median (range)	3.5 (1.0–10.0)	3.0 (1.5–8.0)	4.0 (2.0–8.0)	0.153	0.021
Tumor annularity rate, %					
Median (range)	63.3 (17.6–100)	53.3 (18.8–100)	100 (28.6–100)	0.512	<0.001
Thickness of ulcer, mm					
Median (range)	12.0 (4.0–41.0)	8.0 (4.0–40.0)	9.56 (3.0–26.0)	0.001	0.352
Thickness under the muscular layer, mm					
Median (range)	2.5 (0.1–19.0)	3.0 (0.75–46.0)	4.4 (0.25–20.0)	0.058	0.331
Histologic differentiation					
Well/moderately	108	33	54	0.298	0.298
Poorly/mucinous	5	3	2		
Infiltrating pattern					
Expanding	55	4	4	<0.001	0.382
Invasive	58	32	52		
Tumor depth					
pT3	113	26	44	<0.001	0.486
pT4a	0	10	12		
Nodal status					
pN0	66	16	24	0.002	0.668
pN1	43	12	23		
pN2	4	8	9		
Budding grade					
Grade 1	87	20	35	0.041	0.187
Grade 2	18	12	10		
Grade 3	8	4	11		
Tumor deposits					
+	11	6	6	0.197	0.301
−	102	30	50		
Lymphatic invasion					
+	50	24	37	0.019	0.953
−	63	12	19		
Vascular invasion					
+	64	27	37	0.049	0.364
−	49	9	19		
Perineural invasion					
+	24	15	20	0.015	0.566
−	89	21	36		

ELI, elastic laminal invasion.

The response to CCCM stimulation was significantly higher in SPFs than in SMFs (Fig. 6).

Discussion

In this study, we investigated two types of ELI-positive tumors and first detected the progression-dependent elevation of PEL that was associated with bowel obstruction. Elevation of PEL implied a spread of CMPI toward the luminal surface, and further investigation suggested that the activation of SPFs, which normally reside in the subperitoneal outer area of the colonic wall, contributes to obstruction of the bowel. We have reported that CMPI contributes to tumor progression and metastasis through the interaction of SPFs and cancer cells. Tumors were known to form heterogeneous microenvironments and some of these, including CMPI, promote tumor progression and metastasis.[15–18] However, a progression-dependent alteration of such a tumor microenvironment has not been investigated. In this study, we revealed that a progression-dependent spread of the tumor microenvironment to the shallow layer of the tumor tissue resulted in reduced bowel patency. Our findings first suggest that the tumor-promoting microenvironment can contribute not only to tumor progression or metastasis, but also to the deterioration of clinical findings.

The cancer microenvironment consists of a heterogeneous type of stromal cells, and fibroblasts are one of the major sources.[19] Subperitoneal fibroblasts were reported to be sensitive to CCCM stimulation, and the upregulation of contraction-associated genes, including α-*SMA*, by CCCM was one of the specific features of SPFs.[9] An increase in α-SMA expres-

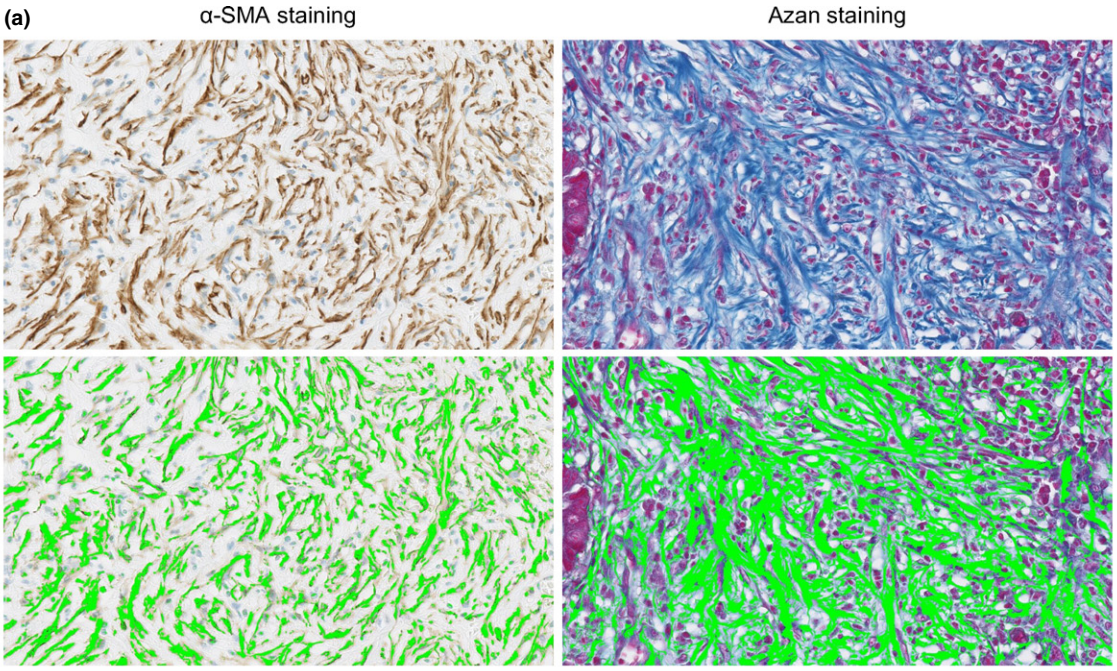

(b) α-SMA staining positive area ratio

Layer	ELI(–)	ELI (+)	
		Non-elevated type	Elevated type
Shallow	11.91% (5.98)	17.68% (5.05)	20.87% (7.05)
Deep	17.68% (6.27)	26.55% (8.89)	28.90% (7.32)
All	14.79% (5.11)	22.11% (5.51)	24.88% (6.02)

(c) Azan staining positive area ratio

Layer	ELI(–)	ELI (+)	
		Non-elevated type	Elevated type
Shallow	32.91% (12.87)	43.83% (14.85)	44.19% (14.20)
Deep	42.24% (11.49)	51.37% (11.64)	50.82% (11.26)
All	37.58% (9.81)	47.60% (11.31)	47.51% (10.88)

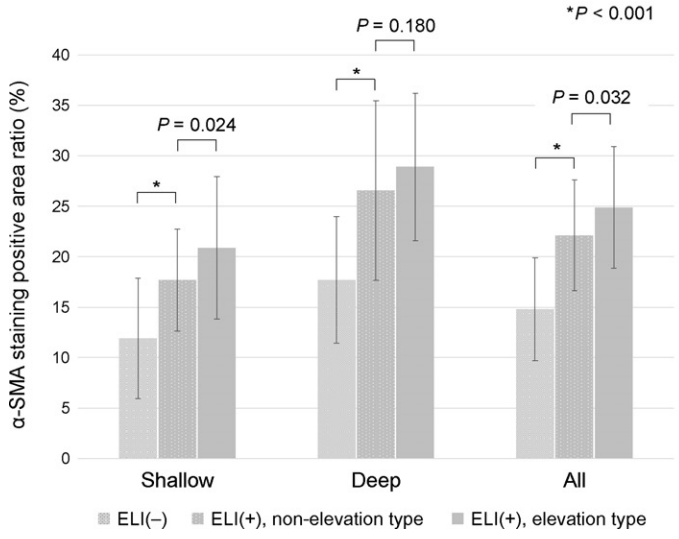

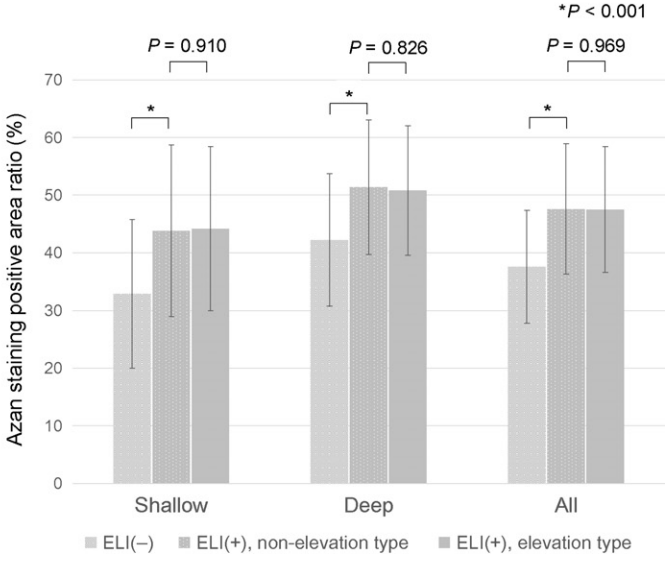

Fig. 4. Association between fibrosis and colon cancer tumor type. α-Smooth muscle actin (α-SMA) staining (×40) and Azan staining (×40) positive areas were successfully detected using morphometric software (a). The α-SMA staining positive area ratio is shown by tumor area (shallow layer, deep layer, and both layers [All]) (b). The Azan staining positive area ratio is also shown (c). Values are mean percentages and those in parentheses are standard deviation. *$P < 0.001$.

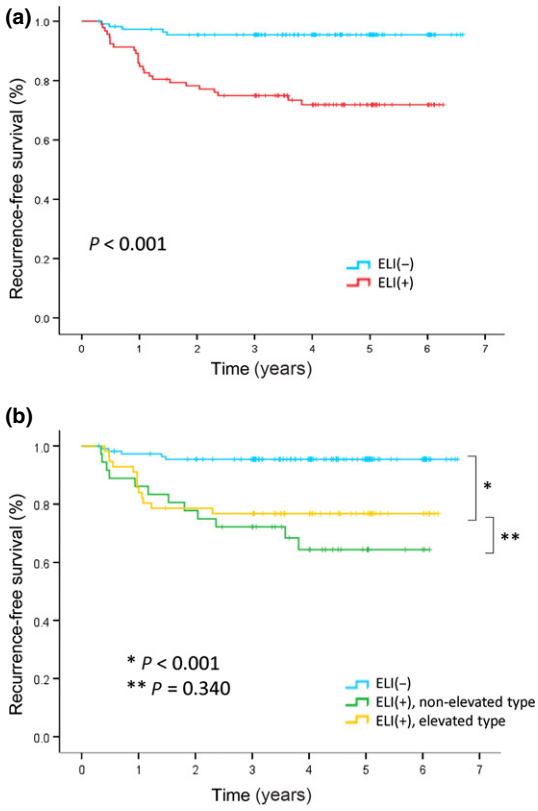

Fig. 5. Kaplan–Meier curves depicting recurrence-free survival of 205 patients who underwent primary resection for pT3 and pT4a colon cancer. (a) Patients were stratified according to elastic laminal invasion (ELI) status. Blue line, ELI-negative cases; red line, ELI-positive cases. (b) Patients were divided into three tumor types. Blue line, ELI-negative type; green, non-elevated type ELI-positive cases; yellow line, elevated type ELI-positive cases.

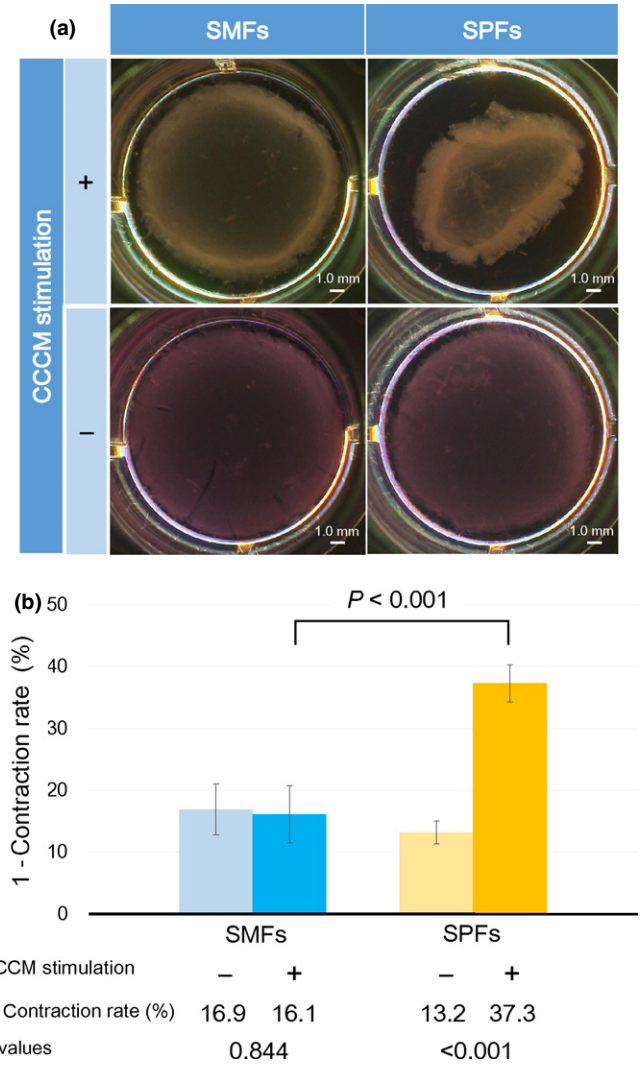

Fig. 6. Contraction assays using submucosal fibroblasts (SMFs) and subperitoneal fibroblasts (SPFs). Gels containing SMFs or SPFs were compared by the presence or absence of cancer cell-conditioned medium (CCCM). (a) Pictures of each gel were taken 48 h after release of each gel from the sides of wells. (b) Contraction rate is shown by bar graph indicating the average value of three gels.

sion was found in CC tissue with strictures and enhanced contractile ability of fibroblasts.[20–22] Concordant with these previous studies, we also found a robust functional contractile ability of SPFs that seemed to be associated with the bowel obstruction. In addition, the spread of CMPI may contribute to the development of clinical findings related to bowel obstruction. However, the spread of this microenvironment did not deteriorate the patient's prognosis. Consequently, the tumor biology would have been already altered by the formation of CMPI, and the spread of CMPI would lead to alteration of tumor morphology.

Morphological alteration in the course of tumor progression has been studied in the early stage of carcinogenesis, as in adenoma–carcinoma sequences and *de novo* cancer. However, there were few studies on the morphological alteration that accompanied the progression of advanced tumor. Recently, we have reported the morphological alteration associated with ELI-positive type invasion.[6] Further detailed analysis in this study revealed that the elevation of the PEL was strongly associated with lateral tumor spread and the resulting increase in tumor annularity rate, which suggested that the spread of CMPI caused morphological alteration. Based on these findings, we propose a model of the morphological alteration that accompanies progression of advanced CC (Fig. 7).

Understanding stromal events may be helpful in the treatment of CRC. More recent research suggests that tumor stroma might be a good target for therapeutic interventions, in particular chemotherapy.[15] For example, it was reported that treatment of pancreatic cancer with nab-paclitaxel reduced the number of cancer-associated fibroblasts in the cancer stroma and improved the response to chemotherapy.[23] Twenty-five percent of patients with uncomplicated CRC with unresectable distant metastasis who underwent chemotherapy required palliative intervention such as bypass surgery, colonic stent, and palliative resection; approximately 80% of these interventions were due to colonic obstruction.[24] We speculate that treatment for tumor stroma improves bowel patency, thereby avoiding stent placement or palliative surgeries that are required for bowel obstruction. Treatments for tumor stroma may be effective in treating patients with unresectable primary CRC to avoid invasive palliative procedures.

The limitation of our study is that there is a difference in the number of H&E and elastica stained slides examined in each case, because we could not adopt the protocol with a predefined number of blocks and sections due to the priority on clinical diagnosis. This might cause a bias in the classification of tumor types.

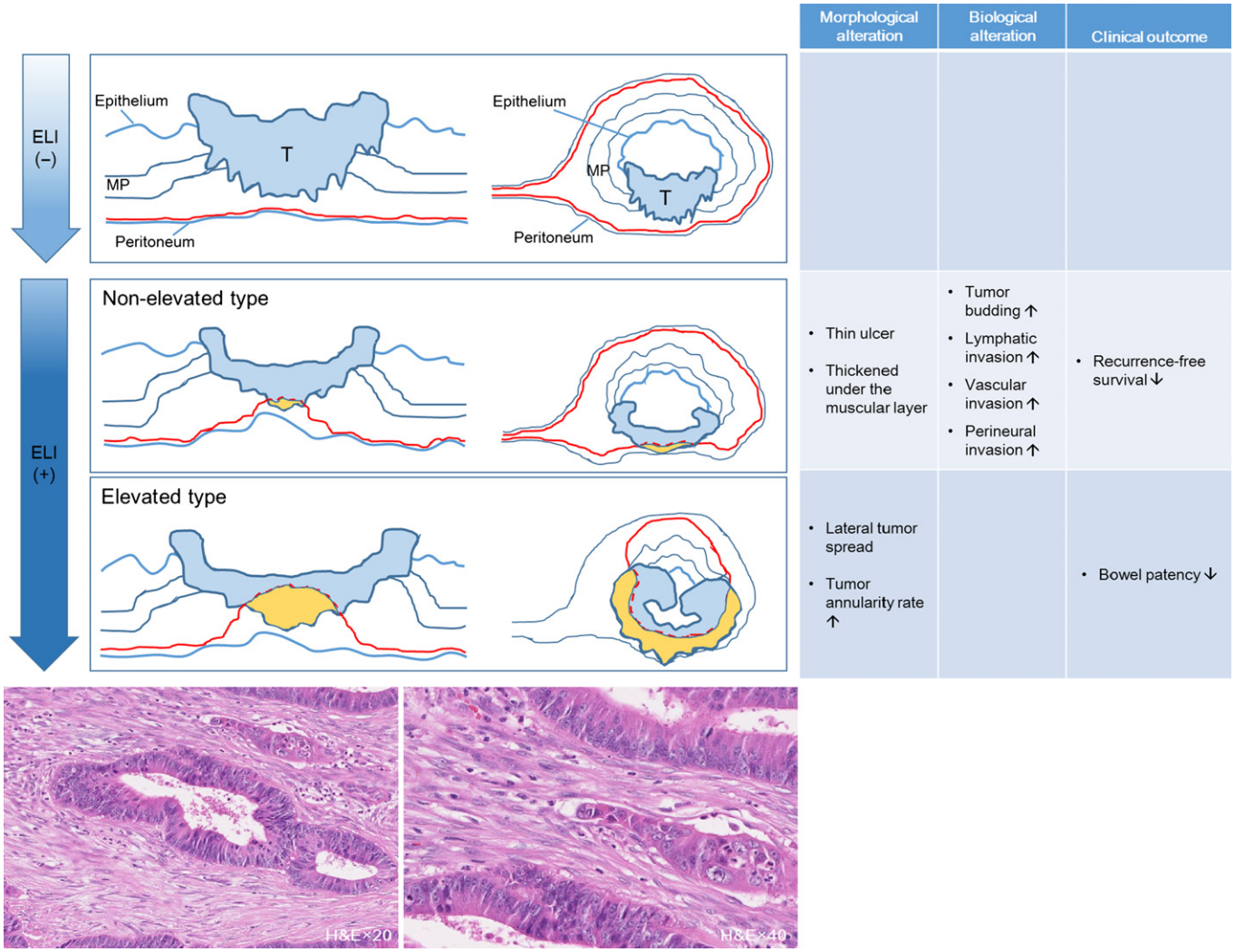

Fig. 7. Proposed model for the tumor progression of colon cancer. Tumor progressed in order of elastic laminal invasion (ELI)-negative type, non-elevated type ELI-positive cases, and elevated type ELI-positive cases. Associations between tumor progression phase and morphological alterations, and biological alterations are described, and the resulting clinical features are shown. The red line represents the peritoneal elastic lamina, and the area filled with yellow represents the cancer microenvironment formed by peritoneal invasion. Histological features of the latter are abundant spindle-shaped fibroblasts and collagen. Higher magnification more clearly revealed spindle-shaped fibroblasts. MP, muscularis propria; T, tumor.

In conclusion, the tumor-promoting microenvironment of CMPI spread into the luminal side of the colonic wall after ELI, and caused bowel obstruction through activation of SPFs. The clinical outcome was affected by CMPI formation, and clinical findings were affected by the spread of CMPI. We are the first group to show that the tumor-promoting microenvironment can spread in the course of tumor progression and can influence physical findings.

Acknowledgment

This study was supported by grants from the Japan Society for the Promotion of Science (Kakenhi 24590458).

Disclosure Statement

The authors have no conflict of interest.

References

1 Ferlay J, Parkin DM, Steliarova-Foucher E. Estimates of cancer incidence and mortality in Europe in 2008. *Eur J Cancer* 2010; **46**: 765–81.
2 Jemal A, Bray F, Center MM, Ferlay J, Ward E, Forman D. Global cancer statistics. *CA Cancer J Clin* 2011; **61**: 69–90.
3 Siegel R, Naishadham D, Jemal A. Cancer statistics, 2012. *CA Cancer J Clin* 2012; **62**: 10–29.
4 Majumdar SR, Fletcher RH, Evans AT. How does colorectal cancer present? Symptoms, duration, and clues to location. *Am J Gastroenterol* 1999; **94**: 3039–45.
5 Hamilton W, Round A, Sharp D, Peters TJ. Clinical features of colorectal cancer before diagnosis: a population-based case–control study. *Br J Cancer* 2005; **93**: 399–405.
6 Kojima M, Nakajima K, Ishii G, Saito N, Ochiai A. Peritoneal elastic laminal invasion of colorectal cancer: the diagnostic utility and clinicopathologic relationship. *Am J Surg Pathol* 2010; **34**: 1351–60.
7 Liang WY, Chang WC, Hsu CY *et al.* Retrospective evaluation of elastic stain in the assessment of serosal invasion of pT3N0 colorectal cancers. *Am J Surg Pathol* 2013; **37**: 1565–70.

8 Yokota M, Kojima M, Nomura S *et al.* Clinical impact of elastic laminal invasion in colon cancer: elastic laminal invasion-positive stage II colon cancer is a high-risk equivalent to stage III. *Dis Colon Rectum* 2014; **57**: 830–8.
9 Kojima M, Higuchi Y, Yokota M *et al.* Human subperitoneal fibroblast and cancer cell interaction creates microenvironment that enhances tumor progression and metastasis. *PLoS One* 2014; **9**: e88018.
10 Sobin LH, Gospodarowicz MK, Wittekind C, eds. *TNM Classification of Malignant Tumors*, 7th edn. West Sussex, UK: Wiley-Blackwell, 2009.
11 Ngo P, Ramalingam P, Phillips JA, Furuta GT. Collagen gel contraction assay. *Methods Mol Biol* 2006; **341**: 103–9.
12 Ueyama T, Yao T, Nakamura K, Enjoji M. Obstructing carcinomas of the colon and rectum: clinicopathologic analysis of 40 cases. *Jpn J Clin Oncol* 1991; **21**: 100–9.
13 Miura S, Kodaira S, Hosoda Y. Immunohistologic analysis of the extracellular matrix components of the fibrous stroma of human colon cancer. *J Surg Oncol* 1993; **53**: 36–42.
14 Miyamoto S, Boku N, Fujii T *et al.* Macroscopic typing with wall stricture sign may reflect tumor behaviors of advanced colorectal cancers. *J Gastroenterol* 2001; **36**: 158–65.
15 Lorusso G, Ruegg C. The tumor microenvironment and its contribution to tumor evolution toward metastasis. *Histochem Cell Biol* 2008; **130**: 1091–103.
16 Alphonso A, Alahari SK. Stromal cells and integrins: conforming to the needs of the tumor microenvironment. *Neoplasia* 2009; **11**: 1264–71.
17 Hanahan D, Weinberg RA. Hallmarks of cancer: the next generation. *Cell* 2011; **144**: 646–74.
18 Quail DF, Joyce JA. Microenvironmental regulation of tumor progression and metastasis. *Nat Med* 2013; **19**: 1423–37.
19 Schmitt-Graff A, Desmouliere A, Gabbiani G. Heterogeneity of myofibroblast phenotypic features: an example of fibroblastic cell plasticity. *Virchows Arch* 1994; **425**: 3–24.
20 Tomasek JJ, Gabbiani G, Hinz B, Chaponnier C, Brown RA. Myofibroblasts and mechano-regulation of connective tissue remodelling. *Nat Rev Mol Cell Biol* 2002; **3**: 349–63.
21 Otranto M, Sarrazy V, Bonte F, Hinz B, Gabbiani G, Desmouliere A. The role of the myofibroblast in tumor stroma remodeling. *Cell Adh Migr* 2012; **6**: 203–19.
22 Hinz B. Matrix mechanics and regulation of the fibroblast phenotype. *Periodontol 2000* 2013; **63**: 14–28.
23 Alvarez R, Musteanu M, Garcia-Garcia E *et al.* Stromal disrupting effects of nab-paclitaxel in pancreatic cancer. *Br J Cancer* 2013; **109**: 926–33.
24 Yun JA, Park Y, Huh JW *et al.* Risk factors for the requirement of surgical or endoscopic interventions during chemotherapy in patients with uncomplicated colorectal cancer and unresectable synchronous metastases. *J Surg Oncol* 2014; **110**: 839–44.